Nucleon pairing correlations and the α cluster preformation probability inside heavy and superheavy nuclei

W. M. Seif*

Department of Physics, Faculty of Science, Cairo University, Giza 12613, Egypt

(Received 23 October 2014; revised manuscript received 11 December 2014; published 27 January 2015)

The presence of paired or unpaired protons and neutrons in the open-shell radioactive α emitter affects the preformation probability of the α cluster inside it. The α-preformation probability inside the odd(Z)-even(N), even(Z)-odd(N), and odd(Z)-odd(N) α emitters is investigated. The study is restricted to those decays with no angular momentum transfer to make a precise prediction about the mere pairing effect. The extended cluster model of α decay and the WKB approximation are used by taking into account the deformation degrees of freedom to carry out the calculations for 105 parent nuclei in the mass region of $A = 175$–289. The α + daughter interaction potential is calculated by using the Hamiltonian energy-density approach in terms of the SLy4 Skyrme-like interaction, then it is implemented to find the average decay width over the different orientations. The half-life of the decay is then estimated and employed in turn to extract the α-preformation probability by taking account of errors on both the released energy and the experimental half-life time. According to the present calculations, it is found that the α cluster preformation probability inside the nuclei which have unpaired nucleons is less than it would be in the neighboring nuclei of the same shell and subshell closures but have no unpaired nucleons. In particular, the effect of the single unpaired neutron in the even(Z)-odd(N) nuclei is slightly larger than that of the single unpaired proton in the odd(Z)-even(N) ones. The effect of the unpaired nucleons appears more clearly in the odd(Z)-odd(N) nuclei which have both an unpaired neutron and an unpaired proton. Based on the obtained results, an empirical pairing term is added to the empirical formula [J. Phys. G **40**, 105102 (2013)] that relates the α cluster preformation probability to the proton and neutron numbers outside the closed shells of the parent nucleus.

DOI: 10.1103/PhysRevC.91.014322 PACS number(s): 23.60.+e, 21.60.Gx, 21.30.Fe, 27.90.+b

I. INTRODUCTION

Towards the goal of investigating a new nuclear island of stability, significant progress has been devoted during past decades to study the synthesis and decays of superheavy nuclei from both experimental and theoretical sides. The theoretical prediction of an island of stability around the closed shells of $Z = 114$ and $N = 184$ [1–3] came in the 1960s. Due to the modern technical facilities, the strenuous experimental and theoretical efforts led to produce successfully synthesized superheavy elements with atomic numbers up to $Z = 118$ at GSI [4–6], the Joint Institute for Nuclear Research-Flerov Laboratory of Nuclear Reactions [7,8], Lawrence Berkeley National Laboratory [9,10] and Rikagaku Kenkyusho [11] in the past two decades. However, the lifetimes of heavy and superheavy nuclei are mainly determined by their main decay mode. The major decay channels of heavy nuclei are the α, β (electron capture) and cluster decays as well as the spontaneous fission. Although the spontaneous fission obviously dominates in the region around Rf and Sg [12], the α-decay mode dominates for the decays of most superheavy nuclei [13]. The heavy-cluster decays, such as the ^{14}C decay of ^{233}Ra [^{233}Ra(^{14}C)], ^{228}Th(^{20}O), ^{231}Pa(^{23}F), ^{236}U(^{24,26}Ne), ^{238}Pu(^{28,30}Mg), ^{238}Pu(^{32}Si), and ^{242}Cm(^{34}Si) compete with the α-decay mode in the region of $Z = 87$–96 [13,14]. The half-life of the radioactive nucleus against a given decay mode is completely determined by the corresponding decay width. In the cluster model, the decay width is well described as a product of three model-dependent quantities, namely, the preformation probability of the emitted clusters inside the decaying nucleus, the assault frequency, and the barrier penetration probability. Commonly, the preformation probability is referred to in the literature as the spectroscopic factor [15–17] or the amount of clustering.

The preformation probability can be calculated microscopically in terms of the probability amplitude of the amount of clustering of the α and daughter as two entities inside the bound parent nucleus [18]. The formation amplitude of the α cluster has been calculated in different studies based on R-matrix approaches [18,19]. By considering the surface nucleons and the Bohr assumption of compound nucleus, the total and formation energy obtained from the binding-energy differences are used in Ref. [20] to find the α cluster preformation factor inside ^{212}Po. Also, the multistep shell model has been employed to improve the calculations of the formation amplitude [21]. In addition to its model dependence, the uncertainty in the determined preformation probability is expected to increase if the involved nuclei are deformed and have larger isospin asymmetry [15,22]. The uncertainty may increase also if there are involved odd nucleon numbers or angular momentum transfer [23,24]. For example, the different predicted values of the α-preformation probability inside ^{212}Po from different models are 0.994 [20], 0.74 [21], 0.54 [20], 0.37 [25], 0.3 [18], 0.22 [25], 0.061 [23], 0.042 [18], 0.035 ± 0.001 [26], 0.019 [16], and 0.000 13 [19]. To avoid possible problems due to the explicit treatment of the detailed nuclear structure in the microscopic calculations [18,27], it is advantageous

*wseif@sci.cu.edu.eg; wseif@yahoo.com

to investigate the preformation probability through its direct relation to the experimental half-life time [15,16,28]. Recently, the α-preformation probability inside even(Z)-even(N) heavy and superheavy nuclei has been studied in Ref. [26] by taking account of the uncertainties in both the released energy and the experimental half-lives as well as the deformations of the daughters. A periodic behavior of the preformation probability as a function of Z and N, characterized by several local maxima and minima, has been observed. The observed minima appeared at the proton-, neutron-shell, and subshell closures of the considered parents. Based on its observed behavior and results [26], an empirical formula has been suggested to give the α-preformation probability in terms of the proton and neutron numbers outside the closed shells of the parent nucleus.

If the parent nucleus has odd nucleon numbers, two more effects must be considered. First, we have to account for the pairing effect. Second, the parent and daughter nuclei may have different nonzero spins and/or a change in their parities. Hence, a rather angular momentum transfer through the outgoing α particle takes place. Like in most nuclear structures and reactions, the nucleon pairing is expected to play a non-negligible effect on the decay process. In the superasymmetric fission model, the shell and pairing effects are included, together, in the suggested values of the zero-point vibration energy E_υ [29], that are obtained from the fit to experimental data on α emitters [30] through its proportionality with the Q value. The zero-point vibration energy is involved in the calculations of the penetration probability via the total energy and the lower and upper turning points included in the action integral [31]. It is also used to find the assault frequency. The influence of the nucleons pairing interaction on the rates of α decay was studied early [32]. The pairing interaction among protons and neutrons that eventually constitute the α particle was found to increase the probability of the α clustering on the nuclear surface [33,34] where the two-neutron and two-proton wave functions interfere constructively [18]. Consequently, this enhances the α-decay width [18] and the giant pairing resonance [18,35]. However, the pairing influences appear also in the pairing energy for the ground state of the nucleus, which affects its binding energy and consequently its α-decay energy Q_α [36]. Recently, the contribution of the pairing correction to the potential barriers and the half-lives for cluster radioactivity has been studied [37] based on a generalized liquid-drop model by adding a phenomenological pairing term. More recently, the total energy among the nucleons inside the nucleus is calculated by taking account of the pairing energy, which was deduced from the separation energies of the nucleons [38]. The formation energy of the α cluster in the nucleus was then deduced from the binding-energy differences. Also, the Skyrme-Hartree-Fock-(HF-) Bogoliubov wave functions, with pairing correlations included, are used to calculate the formation amplitudes and the α-decay probabilities by applying the R-matrix formulation [39]. Too small formation amplitudes have been obtained. It was concluded that, in addition to the pairing correlations included in the Hartree-Fock-Bogoliubov approach, more correlations are still missing, particularly in the nuclear surface, to get improved α particle clustering consistent with data [39]. Furthermore, the α particle formation probabilities have been extracted within the universal decay law approach based on the R matrix [40]. The explanation of the results in terms of the pairing force between the protons and the neutrons that belong to the α particle showed a striking resemblance between the formation probabilities and the pairing gaps, which was extracted from the binding energies [40].

However, the aim of this study is to investigate the influences of the unpaired nucleons on the α-preformation probability inside open-shell nuclei. Towards this goal, the method of deducing the preformation probability by using a semimicroscopic approach based on the SLy4 Skyrme-like interaction within the Wentzel-Kramers-Brillouin (WKB) approximation of the penetration probability is summarized in the next section. The numerical details and results for odd(Z)-even(N), even(Z)-odd(N) and odd(Z)-odd(N) nuclei are given in Sec. III. Only decays with no angular momentum carried by the α particle are considered to extract precise information about the pure pairing effect. The paper ends with the main results and conclusions given in Sec. IV.

II. THEORETICAL BACKGROUND

In the preformed cluster models [41,42], the emitted nucleus and the daughter are supposed to be preborn individually inside the parent nucleus with a definite preformation probability. Subsequently, the emitted particle tries to tunnel through the confining Coulomb barrier between the two formed clusters in the parent. Of course, the shape of the formed daughter cluster and its deformations will affect strongly the tunneling process. The relative orientation of the deformed daughter with respect to the α cluster in the parent nucleus strongly influences the decay width. For a certain orientation angle θ, with respect to the symmetry axis of the deformed daughter, the orientation-dependent α-decay width is given by

$$\Gamma(\theta) = \hbar S_\alpha \nu(\theta) P(\theta). \tag{1}$$

Here, S_α is the preformation probability of the α cluster as a recognizable entity in the parent nucleus. $\nu(\theta)$ is the frequency of assaults of the tunneled α particle on the barrier per second. $P(\theta)$ is the barrier penetrability. The two-dimensional penetrability based on the WKB approximation of the barrier penetration probability is calculated as

$$P(\theta) = \exp\left[-2\int_{R_2(\theta)}^{R_3(\theta)} k(r,\theta)dr\right], \tag{2}$$

with the wave number $k(r,\theta)$ defined as

$$k(r,\theta) = \sqrt{\frac{2\mu}{\hbar^2}|V_T(r,\theta) - Q_\alpha|}. \tag{3}$$

Q_α and $\mu = \frac{m_\alpha m_D}{m_\alpha + m_D}$ represent the experimental released energy in the decay process (in MeV) and the reduced mass of the α + daughter system, respectively. R_i (i = 1–3), in femtometers, are three classical turning points along the decay path. They are obtained by the equation $V_T(r,\theta)|_{r=R_i(\theta)} = Q_\alpha$. After oscillating between $R_1(\theta)$ and $R_2(\theta)$ with the assault frequency ν, the α particle tunnels through the barrier at $R_2(\theta)$ and R_3 [43]. R_3 is rather orientation independent because it always lies in the far tail region [44] of the α + daughter

potential. The total α + daughter interaction energy $V_T(r,\theta)$ reads

$$V_T(r,\theta) = V_N(r,\theta) + V_C(r,\theta) + V_\ell(r), \tag{4}$$

where $V_N(r,\theta)$, $V_C(r,\theta)$, and $V_\ell(r)$ are the nuclear, Coulomb, and the centrifugal contributions, respectively. In terms of the inverse of the time taken for an α particle to traverse the distance between R_1 and R_2, back and forth, we can write the assault frequency as [45,46]

$$\nu(\theta) = T^{-1}(\theta) = \left[\int_{R_1(\theta)}^{R_2(\theta)} \frac{2\mu}{\hbar k(r,\theta)} dr\right]^{-1}. \tag{5}$$

Through this expression, we can easily check that the bound- (quasi-bound-) state wave function of the α cluster verifies the normalization condition in the region between R_1 and R_2 [46]. Now, we can evaluate numerically the angle-averaged decay width as [47]

$$\Gamma = \frac{1}{2}\int_0^\pi \Gamma(\theta)\sin\theta\, d\theta. \tag{6}$$

Finally, the partial half-life ($T_{1/2}$) for the α decay between two definite states of parent and daughter nuclei can be obtained in terms of the calculated decay width (Γ) as

$$T_{1/2} = \frac{\hbar \ln 2}{\Gamma}. \tag{7}$$

However, we can estimate the preformation probability of the α cluster inside the parent nucleus by comparing the calculated half-life, without S_α, with the experimental one [28],

$$S_\alpha = T_{1/2}^{\rm cal}(\text{without } S_\alpha)/T_{1/2}^{\rm exp}. \tag{8}$$

An empirical formula was suggested [26] to relate the α-preformation probability to the numbers of protons and neutrons outside the closed shells of the parent nucleus,

$$S_\alpha = Ae^{-\alpha(Z-Z_0-Z_c)^2}e^{-\beta(N-N_0-N_c)^2}, \tag{9}$$

where Z_0 (N_0) represents the shell and subshell closures of protons (neutrons). Z_c (N_c) defines the number of protons (neutrons) outside the different closed shells at which the preformation probability reaches a local maximum. The dimensionless parameters A, α, and β vary with the shell closures [26].

Returning to the total interaction energy, it is advantageous to use the Hamiltonian energy-density formalism [48] based on a Skyrme interaction. This is because the Skyrme interactions allow the treatment of both the pairing and the shell effects in the nucleus-nucleus interaction potential. Under the frozen density approximation, the real part of the attractive nuclear potential between an emitted α particle and a deformed daughter nucleus reads [26,49,50,51]

$$V_N(R,\theta) = \int H[\rho_{p\alpha}(\vec{r}) + \rho_{pD}(R,\vec{r},\theta), \rho_{n\alpha}(\vec{r}) + \rho_{nD}(R,\vec{r},\theta)] - H_\alpha[\rho_{p\alpha}(\vec{r}), \rho_{n\alpha}(\vec{r})] - H_D[\rho_{pD}(\vec{r}), \rho_{nD}(\vec{r})]d\vec{r}. \tag{10}$$

The separation R (fm) represents here the distance between the centers of mass of the two interacting nuclei. θ is the orientation angle between the symmetry axis direction of the deformed daughter nucleus and the direction of $\vec{R}$. The energy-density functionals of the composite system α and the daughter are denoted, respectively, by H, H_α, and H_D. ρ_{ij} ($i = p,n$ and $j = \alpha, D$) define the frozen density distributions of the protons (p) and neutrons (n) that belong to α and daughter (D) nuclei. The Skyrme energy-density functional $H(\rho)$ is composed of three terms, namely, the kinetic, nuclear, and Coulomb terms,

$$H(\rho_i,\tau_i,\vec{J}_i) = \frac{\hbar^2}{2m}\sum_{i=n,p}\tau_i(\rho_i,\vec{\nabla}\rho_i,\nabla^2\rho_i) + H_{\rm Sky}(\rho_i,\tau_i,\vec{J}_i) + H_{\rm Coul}(\rho_p). \tag{11}$$

Here, τ_i ($i = p,n$) and $\vec{J}_i$ are, respectively, the kinetic energy and the spin-orbit densities of protons and neutrons. Both quantities can be expressed [51] through the extended Thomas-Fermi approximation [49,52] as functions of the local densities and their gradients as well as the form factors of the proton and neutron effective masses $f_i(\vec{r}) = m_i/m_i^{\rm eff}(\vec{r})$. The nuclear part of the energy density $H_{\rm Sky}(\rho_i,\tau_i,\vec{J}_i)$ in terms of the Skyrme nucleon-nucleon interaction which includes zero- and finite-range, density-dependent, effective-mass, and spin-orbit terms as well as the tensor coupling with the spin and gradient terms reads [53]

$$\begin{aligned}
&H_{\rm Sky}(\rho_i,\tau_i,\vec{J}_i)\\
&= \frac{t_0}{2}\left[\left(1+\frac{x_0}{2}\right)\rho^2 - \left(x_0+\frac{1}{2}\right)\sum_{i=p,n}\rho_i^2\right]\\
&+ \frac{t_3\rho^\gamma}{12}\left[\left(1+\frac{x_3}{2}\right)\rho^2 - \left(x_3+\frac{1}{2}\right)\sum_{i=p,n}\rho_i^2\right]\\
&+ \frac{1}{4}\left\{\left[t_1\left(1+\frac{x_1}{2}\right) + t_2\left(1+\frac{x_2}{2}\right)\right]\rho\tau\right.\\
&\left.+ \left[t_2\left(x_2+\frac{1}{2}\right) - t_1\left(x_1+\frac{1}{2}\right)\right]\sum_{i=p,n}\rho_i\tau_i\right\}\\
&+ \frac{1}{16}\left\{\left[3t_1\left(1+\frac{x_1}{2}\right) - t_2\left(1+\frac{x_2}{2}\right)\right](\vec{\nabla}\rho)^2\right.\\
&\left.- \left[3t_1\left(x_1+\frac{1}{2}\right) + t_2\left(x_2+\frac{1}{2}\right)\right]\sum_{i=p,n}(\vec{\nabla}\rho_i)^2\right\}\\
&+ \frac{W_0}{2}\left(\vec{J}\cdot\vec{\nabla}\rho + \sum_{i=p,n}\vec{J}_i\cdot\vec{\nabla}\rho_i\right)\\
&+ \frac{1}{16}\left[(t_1-t_2)\sum_{i=p,n}\vec{J}_i^{\,2} - (t_1x_1+t_2x_2)\vec{J}^{\,2}\right].
\end{aligned} \tag{12}$$

The SLy4 parametrization [γ, t_m, and x_m (m = 0–3)] of the Skyrme nucleon-nucleon interaction and the strength of the spin-orbit interaction (W_0) are given in Ref. [53]. The neutron and proton components of the matter (ρ_i), kinetic energy (τ_i),

and spin-orbit ($\vec{J}_i$) densities can be added simply to give the total ones (ρ, τ, and $\vec{J}$). The Coulomb energy term ($H_{\rm Coul}$) in Eq. (11) consists of two parts, namely, the direct part ($H_C^{\rm dir}$) and the exchange one ($H_C^{\rm exch}$). We can express these two parts as

$$H_{\rm Coul}(\rho_p) = H_C^{\rm dir}(\rho_p) + H_C^{\rm exch}(\rho_p) = \frac{e^2}{2}\rho_p(\vec{r})\int \frac{\rho_p(\vec{r}')}{|\vec{r}-\vec{r}'|}d\vec{r}' - \frac{3e^2}{4}\left(\frac{3}{\pi}\right)^{1/3} \times [\rho_p(\vec{r})]^{4/3}. \quad (13)$$

The Slater approximation [54] has been used here to describe the Coulomb exchange part. Also, we may use the multipole expansion of the deformed density distribution of the daughter nucleus to evaluate the Coulomb direct part [55,56] because of the finite range of the proton-proton Coulomb interaction. The centrifugal part in Eq. (4) $V_\ell(r)$ vanishes if the carried orbital angular momentum (ℓ) by the emitted α particle is zero. To ensure a quasistationary state [57], a renormalization factor is often introduced to the potentials, which are characterized by no repulsive core by applying the Bohr-Sommerfeld quantization [58] and the Wildermuth [59] conditions.

However, the self-consistent HF calculations [60] will be performed by using the SLy4 Skyrme parametrization to get the neutron and proton densities of the α and spherical daughter nuclei. The pairing correlations can be included in these calculations within the BCS approach by means of a constant gap approximation [60]. We may also treat pairing by using constant force or density-dependent zero-range force [53] in the BCS approximation. The densities of the involved deformed daughters will be expressed in the two-parameter Fermi shape,

$$\rho_{n(p)}(r,\theta) = \rho_{0n(p)}(1 + e^{[r-R_{n(p)}(\theta)]/a_{n(p)}})^{-1}, \quad (14)$$

with the half-density radii ($R_{n(p)}$),

$$R_{n(p)}(\theta) = R_{0n(p)}\left[1 + \sum_{i=2,3,4,6}\beta_i Y_{i0}(\theta)\right]. \quad (15)$$

The radii $R_{0n(p)}$ and the diffuseness a parameters of these deformed distributions will be chosen for protons and neutrons so as to reproduce their density distributions obtained from the self-consistent HF + BCS calculations. β_i ($i = 2,3,4,6$) represent the quadrupole, octupole, hexadecapole, and hexacontatetrapole deformations, respectively. The density parameter $\rho_{0n(p)}$ is obtained by normalizing the neutron (proton) density distribution to the number of neutrons (protons) in the nucleus.

III. NUMERICAL RESULTS AND DISCUSSION

The ground-state to ground-state α decays of 105 open-shell odd-A and odd(Z)-odd(N) radioactive nuclei with $80 \leqslant Z \leqslant 114$ and $95 \leqslant N \leqslant 175$ have been studied. For all considered decays, the α emitters and their daughters have the same ground-state spin and parity, and thus the emitted α particle will carry no orbital angular momentum. The neutron and proton density distributions of the involved nuclei are obtained by the Skyrme HF + BCS spherical calculations. The pairing correlations are treated in these calculations by using a constant gap approximation. The densities of the involved deformed daughters have been used in the two-parameter Fermi shape with radius and diffuseness parameters adjusted to reproduce the density distributions from the self-consistent Skyrme HF + BCS calculations. The obtained densities are implemented in turn in the Hamiltonian energy-density scheme Eqs. (10)–(13) to find the total interaction potential of the α + daughter system based on the SLy4 parametrization of the Skyrme interaction. Only for some orientations in a few cases, the lowest point of the pocket in the internal region of the α + daughter potential is obtained above the Q value. In such cases, a normalization factor ($1.01 \leqslant \lambda \leqslant 1.04$) is introduced to account for some uncertainties in the computed nuclear potential. Once the α + daughter interaction potential is calculated at different orientations of the deformed daughter nucleus, it is employed easily to get the barrier penetrability [$P(\theta)$] Eqs. (2) and (3) and the assault frequency [$\nu(\theta)$] Eq. (5). Both $P(\theta)$ and $\nu(\theta)$ are then used to obtain the decay width at a given orientation Eq. (1) without introducing the preformation probability S_α. After orientation averaging over θ [Eq. (6)], the α-decay width is used to find the half-life time of the parent nucleus against its α decay via Eq. (1) without preformation probability. By taking account of the symmetry considerations, the existence of only axial symmetric deformations ($\beta_2, \beta_4, \beta_6$) allows achieving the averaging process Eq. (6) only over the angular range from zero to $\pi/2$ [26]. Finally, we can estimate the preformation probability of the α-daughter clusters inside the parent by comparing its calculated half-life time relative to the corresponding experimental value Eq. (8). The uncertainty range of the obtained preformation probability due to the uncertainties related to the released energy and the experimental half-life time is also estimated for each decay.

Table I summarizes detailed information on the mentioned α decays, the computed half-lives (without the preformation probability), and the estimated preformation probabilities $S_\alpha^{\rm exp}$ [Eq. (8)]. In this table, the third (fourth) column identifies the ground-state spin and parity $J^\pi_{P(D)}$ of the parents (daughters) given in column 1 (2). Listed in the fifth and sixth columns, respectively, are the energy released for each decay [Q_α (MeV)] [61] and the experimental partial half-lives [$T_{1/2}^{\rm exp}$ (s)] [5,62–81]. In the last column of Table I, the references to the experimental half-lives and to the Q_α values which are not taken from Ref. [61] are listed. The calculated quantities given in columns 9 and 10 will be discussed below. Table II shows the multipole ground-state deformations (β_2, β_3, β_4, and β_6) considered in the deformed daughter nuclei [82]. Table I shows that the maximum extracted value of the α-preformation probability $S_\alpha^{\rm exp}$ [Eq. (8)] for the mentioned decays is 0.1294 ± 0.0539 (^{219}Pa). Among the 105 studied cases, 82% yield a preformation probability on the order of 10^{-2} whereas 12% yield smaller $S_\alpha^{\rm exp}$ on the order of 10^{-3}. In a similar study performed on even-even nuclei [26], 72% of the 179 studied nuclei yielded $S_\alpha^{\rm exp}$ on the order of 10^{-2} whereas 25% yielded larger ones on the order of 10^{-1}.

TABLE I. The calculated partial half-lives ($T_{1/2}^{\rm cal}$) of α radioactivity (without the preformation probability) based on the SLy4 Skyrme interaction and the extracted α-preformation probability $S_\alpha^{\rm exp}$ [Eq. (8)]. Presented in the third and fourth columns are the spin and parity of the ground states of parent (column 1) and daughter (column 2) nuclei, respectively. The uncertain spin and/or parity are indicated by the parentheses. The square brackets indicate nonexperimental estimated values [62]. The Q_α values [61] and the experimental partial half-lives are shown in the fifth and sixth columns, respectively. The ninth and tenth columns indicate the estimated preformation probability from the formula given by Eq. (16) and the calculated half-life times based upon these values, respectively. The shown references in the last column are for the experimental partial half-life times $T_{1/2}^{\rm exp}$ and the Q_α values (for the cases in which they are not from Ref. [61]).

Parent	Daughter	J_P^π	J_D^π	Q_α (MeV)	$T_{1/2}^{\rm exp}$ (s)	$T_{1/2}^{\rm cal}$ (without S_α) (s)	$S_\alpha^{\rm exp}$ [Eq. (8)]	S_α [Eq.(16)]	$T_{1/2}^{\rm cal}$ (s) (by using S_α [Eq. (16)])	References
^{175}Hg	^{171}Pt	$(7/2^-)$	$7/2^-$	7.072 ± 0.005	$(1.060 \pm 0.040) \times 10^{-2}$	$4.184^{+0.182}_{-0.126} \times 10^{-4}$	0.0398 ± 0.0030	0.0484	$0.841^{+0.038}_{-0.026} \times 10^{-2}$	[62]
^{179}Hg	^{175}Pt	$7/2^-$	$(7/2^-)$	6.351 ± 0.030	1.410 ± 0.120	$0.117^{+0.038}_{-0.027}$	0.0895 ± 0.0307	0.0167	$6.998^{+2.273}_{-1.615}$	[63]
^{183}Hg	^{179}Pt	$1/2^-$	$1/2^-$	6.038 ± 0.004	80.300 ± 15.000	$0.930^{+0.036}_{-0.042}$	0.0121 ± 0.0027	0.0075	$124.209^{+4.808}_{-5.609}$	[64]
^{185}Hg	^{181}Pt	$1/2^-$	$1/2^-$	5.774 ± 0.005	$(8.180 \pm 1.370) \times 10^2$	$14.010^{+0.801}_{-0.484}$	0.0180 ± 0.0038	0.0094	$14.849^{+0.850}_{-0.513} \times 10^2$	[64]
^{177}Tl	^{173}Au	$(1/2^+)$	$(1/2^+)$	7.067 ± 0.007	0.018 ± 0.005	$8.842^{+0.460}_{-0.486} \times 10^{-4}$	0.0539 ± 0.0176	0.0404	$0.022^{+0.001}_{-0.001}$	[62]
^{179}Tl	^{175}Au	$1/2^+$	$1/2^+$	6.710 ± 0.005	0.265 ± 0.010	$1.409^{+0.140}_{-0.060} \times 10^{-2}$	0.0549 ± 0.0058	0.0257	$0.548^{+0.054}_{-0.023}$	[65]
^{191}Pb	^{187}Hg	$(3/2^-)$	$3/2^{(-)}$	5.460 ± 0.040	$(6.138 \pm 0.369) \times 10^5$	$7.415^{+4.525}_{-2.835} \times 10^3$	0.0139 ± 0.0068	0.0335	$2.215^{+1.352}_{-0.847} \times 10^5$	[66]
^{191}Po	^{187}Pb	$(3/2^-)$	$3/2^-$	7.493 ± 0.005	$(2.200 \pm 0.100) \times 10^{-2}$	$5.157^{+0.238}_{-0.208} \times 10^{-4}$	0.0236 ± 0.0021	0.0445	$1.158^{+0.053}_{-0.047} \times 10^{-2}$	[62]
^{193}Po	^{189}Pb	$(3/2^-)$	$3/2^-$	7.094 ± 0.004	0.370 ± 0.040	$1.080^{+0.034}_{-0.036} \times 10^{-2}$	0.0296 ± 0.0041	0.0518	$0.209^{+0.007}_{-0.007}$	[62]
^{195}Po	^{191}Pb	$(3/2^-)$	$(3/2^-)$	6.750 ± 0.003	4.640 ± 0.090	$0.185^{+0.007}_{-0.004}$	0.0402 ± 0.0020	0.0555	$3.333^{+0.126}_{-0.072}$	[62]
^{197}Po	^{193}Pb	$(3/2^-)$	$(3/2^-)$	6.412 ± 0.003	$(1.253 \pm 0.220) \times 10^2$	$3.802^{+0.107}_{-0.096}$	0.0315 ± 0.0063	0.0548	$0.694^{+0.020}_{-0.018} \times 10^2$	[62][a]
^{199}Po	^{195}Pb	$[3/2^-]$	$[3/2^-]$	6.074 ± 0.002	$(2.740 \pm 0.464) \times 10^3$	$1.021^{+0.029}_{-0.007} \times 10^2$	0.0389 ± 0.0072	0.0495	$2.061^{+0.059}_{-0.014} \times 10^3$	[64]
^{201}Po	^{197}Pb	$3/2^-$	$3/2^-$	5.799 ± 0.002	$(5.740 \pm 1.080) \times 10^4$	$1.809^{+0.055}_{-0.012} \times 10^3$	0.0332 ± 0.0068	0.0407	$4.445^{+0.136}_{-0.030} \times 10^4$	[64]
^{205}Po	^{201}Pb	$5/2^-$	$5/2^-$	5.325 ± 0.010	$(1.690 \pm 0.494) \times 10^7$	$4.477^{+0.389}_{-0.713} \times 10^5$	0.0290 ± 0.0117	0.0186	$2.411^{+0.210}_{-0.384} \times 10^7$	[62][a]
^{207}Po	^{203}Pb	$5/2^-$	$5/2^-$	5.216 ± 0.003	$(9.940 \pm 0.948) \times 10^7$	$1.559^{+0.059}_{-0.036} \times 10^6$	0.0160 ± 0.0020	0.0084	$18.603^{+0.703}_{-0.434} \times 10^7$	[64]
^{213}Po	^{209}Pb	$9/2^+$	$9/2^+$	8.536 ± 0.003	$(3.720 \pm 0.020) \times 10^{-6}$	$1.134^{+0.018}_{-0.010} \times 10^{-7}$	0.0306 ± 0.0005	0.0284	$3.994^{+0.063}_{-0.034} \times 10^{-6}$	[62]
^{215}Po	^{211}Pb	$9/2^+$	$9/2^+$	7.526 ± 0.001	$(1.781 \pm 0.004) \times 10^{-3}$	$9.362^{+0.131}_{-0.108} \times 10^{-5}$	0.0526 ± 0.0008	0.0507	$1.845^{+0.026}_{-0.021} \times 10^{-3}$	[62]
^{217}Po	^{213}Pb	$(9/2^+)$	$(9/2^+)$	6.662 ± 0.002	1.514 ± 0.026	$7.985^{+0.115}_{-0.151} \times 10^{-2}$	0.0527 ± 0.0018	0.0733	$1.032^{+0.015}_{-0.020}$	[62]
^{196}At	^{192}Bi	(3^+)	(3^+)	7.198 ± 0.004	0.350 ± 0.090	$8.567^{+0.279}_{-0.285} \times 10^{-3}$	0.0264 ± 0.0076	0.0572	$0.150^{+0.005}_{-0.005}$	[67]
^{197}At	^{193}Bi	$(9/2^-)$	$(9/2^-)$	7.100 ± 0.050	0.354 ± 0.017	$1.815^{+0.953}_{-0.610} \times 10^{-2}$	0.0573 ± 0.0248	0.0707	$0.257^{+0.135}_{-0.086}$	[67]
^{198}At	^{194}Bi	(3^+)	(3^+)	6.890 ± 0.002	3.000 ± 0.100	$0.103^{+0.002}_{-0.002}$	0.0344 ± 0.0018	0.0562	$1.833^{+0.036}_{-0.036}$	[67]
^{199}At	^{195}Bi	$(9/2^-)$	$(9/2^-)$	6.777 ± 0.001	7.020 ± 0.120	$0.267^{+0.003}_{-0.004}$	0.0380 ± 0.0011	0.0680	$3.926^{+0.044}_{-0.059}$	[62]
^{200}At	^{196}Bi	(3^+)	(3^+)	6.596 ± 0.001	43.200 ± 0.900	$1.328^{+0.010}_{-0.018}$	0.0307 ± 0.0010	0.0500	$26.562^{+0.194}_{-0.368}$	[62]
^{201}At	^{197}Bi	$(9/2^-)$	$(9/2^-)$	6.473 ± 0.002	85.200 ± 1.600	$4.037^{+0.055}_{-0.099}$	0.0472 ± 0.0018	0.0604	$66.800^{+0.914}_{-1.630}$	[62]
^{202}At	^{198}Bi	$(2^+,3^+)$	$(2^+,3^+)$	6.354 ± 0.001	$(5.163 \pm 1.004) \times 10^2$	$12.100^{+0.092}_{-0.008}$	0.0245 ± 0.0049	0.0397	$3.048^{+0.023}_{-0.002} \times 10^2$	[62][a]
^{203}At	^{199}Bi	$9/2^-$	$9/2^-$	6.210 ± 0.001	$(1.430 \pm 0.144) \times 10^3$	$63.100^{+0.238}_{-0.007}$	0.0447 ± 0.0046	0.0495	$1.275^{+0.005}_{-0.000} \times 10^3$	[64]
^{204}At	^{200}Bi	7^+	7^+	6.070 ± 0.001	$(14.500 \pm 0.827) \times 10^3$	$2.567^{+0.045}_{-0.013} \times 10^2$	0.0179 ± 0.0012	0.0270	$9.492^{+0.166}_{-0.048} \times 10^3$	[64]

TABLE I. (*Continued.*)

Parent	Daughter	J_P^π	J_D^π	Q_α (MeV)	$T_{1/2}^{\exp}$ (s)	$T_{1/2}^{\mathrm{cal}}$ (without S_α) (s)	$S_\alpha^{\exp}$ [Eq. (8)]	S_α [Eq.(16)]	$T_{1/2}^{\mathrm{cal}}$ (s) (by using S_α [Eq. (16)])	References
^{205}At	^{201}Bi	$9/2^-$	$9/2^-$	6.020 ± 0.002	$(1.570 \pm 0.316) \times 10^4$	$422.033^{+5.130}_{-9.167}$	0.0280 ± 0.0061	0.0372	$1.136^{+0.014}_{-0.025} \times 10^4$	[64]
^{207}At	^{203}Bi	$9/2^-$	$9/2^-$	5.872 ± 0.003	$(7.530 \pm 0.892) \times 10^4$	$1.836^{+0.086}_{-0.058} \times 10^3$	0.0250 ± 0.0039	0.0252	$7.274^{+0.341}_{-0.230} \times 10^4$	[64]
^{208}At	^{204}Bi	6^+	6^+	5.751 ± 0.002	$(1.082 \pm 0.138) \times 10^6$	$5.496^{+0.070}_{-0.166} \times 10^3$	0.0051 ± 0.0008	0.0021	$2.572^{+0.033}_{-0.078} \times 10^6$	[62][a]
^{209}At	^{205}Bi	$9/2^-$	$9/2^-$	5.757 ± 0.002	$(4.750 \pm 0.581) \times 10^5$	$6.090^{+0.144}_{-0.155} \times 10^3$	0.0130 ± 0.0019	0.0151	$4.045^{+0.096}_{-0.103} \times 10^5$	[64]
^{211}At	^{207}Bi	$9/2^-$	$9/2^-$	5.982 ± 0.001	$(6.210 \pm 0.013) \times 10^4$	$4.315^{+0.028}_{-0.124} \times 10^2$	0.0069 ± 0.0001	0.0092	$4.706^{+0.030}_{-0.135} \times 10^4$	[64]
^{213}At	^{209}Bi	$9/2^-$	$9/2^-$	9.254 ± 0.005	$(1.250 \pm 0.060) \times 10^{-7}$	$4.410^{+0.121}_{-0.117} \times 10^{-9}$	0.0354 ± 0.0027	0.0244	$1.804^{+0.049}_{-0.048} \times 10^{-7}$	[64]
^{214}At	^{210}Bi	1^-	1^-	8.987 ± 0.004	$(5.580 \pm 0.100) \times 10^{-7}$	$1.831^{+0.041}_{-0.035} \times 10^{-8}$	0.0329 ± 0.0013	0.0262	$6.997^{+0.157}_{-0.134} \times 10^{-7}$	[62]
^{215}At	^{211}Bi	$9/2^-$	$9/2^-$	8.178 ± 0.004	$(1.000 \pm 0.200) \times 10^{-4}$	$2.505^{+0.055}_{-0.037} \times 10^{-6}$	0.0263 ± 0.0057	0.0479	$0.523^{+0.012}_{-0.008} \times 10^{-4}$	[62]
^{216}At	^{212}Bi	$1^{(-)}$	$1^{(-)}$	7.950 ± 0.003	$(3.000 \pm 0.300) \times 10^{-4}$	$1.090^{+0.037}_{-0.017} \times 10^{-5}$	0.0371 ± 0.0046	0.0519	$2.100^{+0.071}_{-0.033} \times 10^{-4}$	[62]
^{217}At	^{213}Bi	$9/2^-$	$9/2^-$	7.201 ± 0.001	$(3.230 \pm 0.040) \times 10^{-2}$	$2.913^{+0.033}_{-0.022} \times 10^{-3}$	0.0904 ± 0.0020	0.0781	$3.731^{+0.042}_{-0.028} \times 10^{-2}$	[62]
^{218}At	^{214}Bi	$[1^-]$	1^-	6.874 ± 0.003	1.500 ± 0.300	$4.243^{+0.173}_{-0.090} \times 10^{-2}$	0.0299 ± 0.0069	0.0824	$0.515^{+0.021}_{-0.011}$	[62]
^{219}At	^{215}Bi	$(9/2^-)$	$9/2^-$	6.324 ± 0.015	56.000 ± 3.000	$6.811^{+1.020}_{-0.985}$	0.1233 ± 0.0245	0.1095	$62.188^{+9.313}_{-8.994}$	[62]
^{195}Rn	^{191}Po	$(3/2^-)$	$(3/2^-)$	7.690 ± 0.050	0.007 ± 0.003	$2.255^{+1.000}_{-0.690} \times 10^{-4}$	0.0485 ± 0.0329	0.0694	$0.003^{+0.001}_{-0.001}$	[62]
^{197}Rn	^{193}Po	$(3/2^-)$	$(3/2^-)$	7.411 ± 0.007	0.054 ± 0.006	$7.852^{+0.433}_{-0.420} \times 10^{-4}$	0.0148 ± 0.0024	0.0745	$0.011^{+0.001}_{-0.001}$	[62]
^{199}Rn	^{195}Po	$(3/2^-)$	$(3/2^-)$	7.140 ± 0.050	0.590 ± 0.030	$4.099^{+2.131}_{-1.405} \times 10^{-2}$	0.0774 ± 0.0339	0.0737	$0.556^{+0.289}_{-0.191}$	[62]
^{201}Rn	^{197}Po	$(3/2^-)$	$(3/2^-)$	6.861 ± 0.002	7.000 ± 0.400	$0.411^{+0.009}_{-0.006}$	0.0592 ± 0.0045	0.0672	$6.120^{+0.134}_{-0.089}$	[62]
^{203}Rn	^{199}Po	$[3/2^-]$	$[3/2^-]$	6.630 ± 0.002	44.000 ± 2.000	$3.166^{+0.074}_{-0.035}$	0.0726 ± 0.0045	0.0560	$56.578^{+1.322}_{-0.625}$	[62]
^{207}Rn	^{203}Po	$5/2^-$	$5/2^-$	6.251 ± 0.002	$(2.640 \pm 0.381) \times 10^3$	$1.055^{+0.027}_{-0.013} \times 10^2$	0.0412 ± 0.0067	0.0278	$3.796^{+0.097}_{-0.047} \times 10^3$	[64]
^{209}Rn	^{205}Po	$5/2^-$	$5/2^-$	6.156 ± 0.002	$(1.010 \pm 0.123) \times 10^4$	$2.500^{+0.041}_{-0.069} \times 10^2$	0.0251 ± 0.0036	0.0148	$1.687^{+0.028}_{-0.047} \times 10^4$	[64]
^{215}Rn	^{211}Po	$9/2^+$	$9/2^+$	8.839 ± 0.008	$(2.300 \pm 0.100) \times 10^{-6}$	$9.760^{+0.567}_{-0.430} \times 10^{-8}$	0.0429 ± 0.0040	0.0386	$2.526^{+0.147}_{-0.111} \times 10^{-6}$	[62]
^{217}Rn	^{213}Po	$9/2^+$	$9/2^+$	7.887 ± 0.003	$(5.400 \pm 0.500) \times 10^{-4}$	$4.328^{+0.083}_{-0.049} \times 10^{-5}$	0.0813 ± 0.0087	0.0678	$6.385^{+0.122}_{-0.072} \times 10^{-4}$	[62]
^{199}Fr	^{195}At	$[1/2^+]$	$1/2^+$	7.810 ± 0.004	$4.500^{+3.100}_{-1.300} \times 10^{-3}$	$2.066^{+0.914}_{-0.636} \times 10^{-4}$	0.0560 ± 0.0372	0.0867	$2.382^{+1.054}_{-0.733} \times 10^{-3}$	[68]
^{200}Fr	^{196}At	(3^+)	(3^+)	7.620 ± 0.050	0.046 ± 0.021	$8.754^{+4.067}_{-2.677} \times 10^{-4}$	0.0302 ± 0.0211	0.0722	$0.012^{+0.006}_{-0.004}$	[67,69][b]
^{201}Fr	^{197}At	$(9/2^-)$	$(9/2^-)$	7.520 ± 0.050	0.060 ± 0.011	$1.807^{+0.846}_{-0.591} \times 10^{-3}$	0.0356 ± 0.0185	0.0834	$0.022^{+0.010}_{-0.007}$	[67,70,71][b]
^{202}Fr	^{198}At	(3^+)	(3^+)	7.389 ± 0.004	0.287 ± 0.097	$4.896^{+0.169}_{-0.150} \times 10^{-3}$	0.0195 ± 0.0071	0.0650	$0.073^{+0.003}_{-0.002}$	[67,70,72][b]
^{203}Fr	^{199}At	$[9/2^-]$	$(9/2^-)$	7.275 ± 0.004	0.550 ± 0.010	$3.397^{+0.116}_{-0.092} \times 10^{-2}$	0.0620 ± 0.0030	0.0742	$0.458^{+0.016}_{-0.012}$	[62]
^{204}Fr	^{200}At	(3^+)	(3^+)	7.170 ± 0.003	1.750 ± 0.260	$6.677^{+0.102}_{-0.208} \times 10^{-2}$	0.0388 ± 0.0067	0.0526	$1.269^{+0.019}_{-0.040}$	[62]
^{205}Fr	^{201}At	$(9/2^-)$	$(9/2^-)$	7.055 ± 0.002	3.820 ± 0.060	$0.173^{+0.002}_{-0.003}$	0.0452 ± 0.0014	0.0608	$2.846^{+0.033}_{-0.049}$	[62]
^{206}Fr	^{202}At	$(2^+,3^+)$	$(2^+,3^+)$	6.923 ± 0.004	18.100 ± 0.852	$5.246^{+0.176}_{-0.166} \times 10^{-1}$	0.0291 ± 0.0023	0.0373	$14.050^{+0.471}_{-0.445}$	[64]
^{207}Fr	^{203}At	$9/2^-$	$9/2^-$	6.893 ± 0.020	14.800 ± 0.100	$0.687^{+0.146}_{-0.110}$	0.0477 ± 0.0090	0.0457	$15.037^{+3.196}_{-2.408}$	[62]
^{208}Fr	^{204}At	7^+	7^+	6.785 ± 0.024	59.100 ± 0.300	$1.356^{+0.320}_{-0.275}$	0.0234 ± 0.0052	0.0216	$62.871^{+14.837}_{-12.750}$	[62]
^{209}Fr	^{205}At	$9/2^-$	$9/2^-$	6.777 ± 0.004	50.000 ± 0.300	$1.772^{+0.032}_{-0.085}$	0.0349 ± 0.0014	0.0311	$56.973^{+1.029}_{-2.733}$	[62]

TABLE I. (*Continued.*)

Parent	Daughter	J_P^π	J_D^π	Q_α (MeV)	$T_{1/2}^{\exp}$ (s)	$T_{1/2}^{\mathrm{cal}}$ (without S_α) (s)	$S_\alpha^{\exp}$ [Eq. (8)]	S_α [Eq.(16)]	$T_{1/2}^{\mathrm{cal}}$ (s) (by using S_α [Eq. (16)])	References
^{211}Fr	^{207}At	$9/2^-$	$9/2^-$	6.662 ± 0.003	186.000 ± 1.200	$4.444^{+0.105}_{-0.106}$	0.0239 ± 0.0007	0.0186	$238.418^{+5.633}_{-5.687}$	[62]
^{213}Fr	^{209}At	$9/2^-$	$9/2^-$	6.905 ± 0.001	34.820 ± 0.140	$4.183^{+0.044}_{-0.037} \times 10^{-1}$	0.0120 ± 0.0002	0.0114	$36.564^{+0.385}_{-0.323}$	[62]
^{215}Fr	^{211}At	$9/2^-$	$9/2^-$	9.540 ± 0.007	$(8.600 \pm 0.500) \times 10^{-8}$	$4.570^{+0.202}_{-0.122} \times 10^{-9}$	0.0539 ± 0.0050	0.0301	$15.168^{+0.670}_{-0.405} \times 10^{-8}$	[62]
^{216}Fr	^{212}At	(1^-)	(1^-)	9.174 ± 0.003	$(7.000 \pm 0.200) \times 10^{-7}$	$3.385^{+0.081}_{-0.057} \times 10^{-8}$	0.0486 ± 0.0024	0.0338	$10.003^{+0.239}_{-0.168} \times 10^{-7}$	[62]
^{217}Fr	^{213}At	$9/2^-$	$9/2^-$	8.469 ± 0.004	$(2.200 \pm 0.500) \times 10^{-5}$	$2.181^{+0.052}_{-0.049} \times 10^{-6}$	0.1052 ± 0.0262	0.0588	$3.708^{+0.088}_{-0.083} \times 10^{-5}$	[64]
^{218}Fr	^{214}At	1^-	1^-	8.014 ± 0.002	$(1.000 \pm 0.600) \times 10^{-3}$	$4.370^{+0.079}_{-0.033} \times 10^{-5}$	0.0692 ± 0.0421	0.0659	$0.663^{+0.012}_{-0.005} \times 10^{-3}$	[62]
^{219}Fr	^{215}At	$9/2^-$	$9/2^-$	7.449 ± 0.002	$(2.000 \pm 0.200) \times 10^{-2}$	$2.467^{+0.058}_{-0.027} \times 10^{-3}$	0.1256 ± 0.0147	0.0957	$2.577^{+0.061}_{-0.028} \times 10^{-2}$	[62]
^{203}Ra	^{199}Rn	$(3/2^-)$	$(3/2^-)$	7.740 ± 0.050	0.056 ± 0.034	$3.636^{+1.673}_{-1.072} \times 10^{-4}$	0.0135 ± 0.0106	0.0801	$0.005^{+0.002}_{-0.001}$	[67,70][b]
^{205}Ra	^{201}Rn	$(3/2^-)$	$(3/2^-)$	7.490 ± 0.050	0.220 ± 0.050	$5.612^{+2.732}_{-1.871} \times 10^{-3}$	0.0315 ± 0.0176	0.0671	$0.084^{+0.041}_{-0.028}$	[62]
^{209}Ra	^{205}Rn	$5/2^-$	$5/2^-$	7.143 ± 0.003	4.710 ± 0.080	$0.139^{+0.005}_{-0.004}$	0.0296 ± 0.0015	0.0346	$4.023^{+0.145}_{-0.116}$	[62]
^{211}Ra	^{207}Rn	$5/2^{(-)}$	$5/2^-$	7.042 ± 0.003	13.200 ± 1.400	$0.333^{+0.010}_{-0.010}$	0.0256 ± 0.0035	0.0195	$17.050^{+0.512}_{-0.512}$	[62]
^{217}Ra	^{213}Rn	$(9/2^+)$	$[9/2^+]$	9.161 ± 0.006	$(1.600 \pm 0.200) \times 10^{-6}$	$8.062^{+0.065}_{-0.436} \times 10^{-8}$	0.0502 ± 0.0078	0.0462	$1.747^{+0.014}_{-0.094} \times 10^{-6}$	[73]
^{215}Ac	^{211}Fr	$9/2^-$	$9/2^-$	7.746 ± 0.003	$0.170^{+0.010}_{-0.010}$	$2.868^{+0.105}_{-0.046} \times 10^{-3}$	0.0171 ± 0.0015	0.0126	$0.228^{+0.008}_{-0.004}$	[62]
^{217}Ac	^{213}Fr	$9/2^-$	$9/2^-$	9.832 ± 0.010	$(6.900 \pm 0.400) \times 10^{-8}$	$4.813^{+0.128}_{-0.293} \times 10^{-9}$	0.0690 ± 0.0070	0.0332	$14.480^{+0.385}_{-0.882} \times 10^{-8}$	[62]
^{218}Ac	^{214}Fr	$[1^-]$	(1^-)	9.380 ± 0.050	$(1.080 \pm 0.090) \times 10^{-6}$	$4.650^{+1.486}_{-1.157} \times 10^{-8}$	0.0459 ± 0.0161	0.0379	$1.227^{+0.392}_{-0.305} \times 10^{-6}$	[62]
^{219}Ac	^{215}Fr	$9/2^-$	$9/2^-$	8.830 ± 0.050	$(1.180 \pm 0.150) \times 10^{-5}$	$1.256^{+0.459}_{-0.332} \times 10^{-6}$	0.1180 ± 0.0485	0.0650	$1.933^{+0.707}_{-0.511} \times 10^{-5}$	[62]
^{221}Ac	^{217}Fr	$[9/2^-]$	$9/2^-$	7.780 ± 0.050	0.052 ± 0.002	$1.506^{+0.661}_{-0.499} \times 10^{-3}$	0.0310 ± 0.0123	0.1058	$0.014^{+0.006}_{-0.005}$	[62]
^{222}Ac	^{218}Fr	1^-	1^-	7.137 ± 0.002	5.000 ± 0.500	$3.377^{+0.037}_{-0.072} \times 10^{-1}$	0.0680 ± 0.0079	0.1156	$2.921^{+0.032}_{-0.062}$	[62]
^{227}Ac	^{223}Fr	$3/2^-$	$3/2^{(-)}$	5.042 ± 0.0001	$(53.424 \pm 13.944) \times 10^9$	$18.928^{+0.051}_{-0.046} \times 10^7$	0.0038 ± 0.0010	0.1936	$0.978^{+0.003}_{-0.002} \times 10^9$	[62][a]
^{219}Th	^{215}Ra	$[9/2^+]$	$[9/2^+]$	9.510 ± 0.050	$(1.050 \pm 0.030) \times 10^{-6}$	$5.546^{+1.728}_{-1.430} \times 10^{-8}$	0.0547 ± 0.0166	0.0489	$1.134^{+0.353}_{-0.292} \times 10^{-6}$	[62]
^{217}Pa	^{213}Ac	$[9/2^-]$	$[9/2^-]$	8.489 ± 0.004	$(3.480 \pm 0.090) \times 10^{-3}$	$8.566^{+0.251}_{-0.321} \times 10^{-5}$	0.0246 ± 0.0015	0.0119	$7.211^{+0.211}_{-0.270} \times 10^{-3}$	[62]
^{219}Pa	^{215}Ac	$9/2^-$	$9/2^-$	10.080 ± 0.050	$(5.300 \pm 1.000) \times 10^{-8}$	$6.110^{+1.772}_{-1.359} \times 10^{-9}$	0.1294 ± 0.0539	0.0326	$18.770^{+5.444}_{-4.175} \times 10^{-8}$	[62]
^{220}Pa	^{216}Ac	$[1^-]$	$[1^-]$	9.830 ± 0.050	$(7.800 \pm 1.600) \times 10^{-7}$	$2.112^{+0.647}_{-0.493} \times 10^{-8}$	0.0309 ± 0.0136	0.0368	$5.740^{+1.758}_{-1.340} \times 10^{-7}$	[74]
^{221}Pa	^{217}Ac	$9/2^-$	$9/2^-$	9.250 ± 0.050	$(5.900 \pm 1.700) \times 10^{-6}$	$5.201^{+1.824}_{-1.343} \times 10^{-7}$	0.1090 ± 0.0582	0.0643	$8.090^{+2.837}_{-2.089} \times 10^{-6}$	[62]
^{223}Pa	^{219}Ac	$[9/2^-]$	$9/2^-$	8.330 ± 0.050	$(5.000 \pm 1.000) \times 10^{-3}$	$1.128^{+0.458}_{-0.336} \times 10^{-4}$	0.0264 ± 0.0132	0.1051	$1.073^{+0.436}_{-0.320} \times 10^{-3}$	[75,76][b]
^{227}Pa	^{223}Ac	$(5/2^-)$	$(5/2^-)$	6.580 ± 0.002	$(2.298 \pm 0.018) \times 10^3$	$14.470^{+0.198}_{-0.383}$	0.0063 ± 0.0002	0.1805	$0.080^{+0.001}_{-0.002} \times 10^3$	[62]
^{231}Pa	^{227}Ac	$3/2^-$	$3/2^-$	5.150 ± 0.001	$(10.340 \pm 0.035) \times 10^{11}$	$4.864^{+0.091}_{-0.082} \times 10^8$	0.0005	0.1805	$0.027^{+0.001}_{-0.001} \times 10^{11}$	[62]
^{229}U	^{225}Th	$(3/2^+)$	$(3/2^+)$	6.475 ± 0.003	$(1.740 \pm 0.090) \times 10^4$	$1.101^{+0.033}_{-0.043} \times 10^2$	0.0063 ± 0.0005	0.1796	$0.061^{+0.002}_{-0.002} \times 10^4$	[62][a]
^{233}U	^{229}Th	$5/2^+$	$5/2^+$	4.909 ± 0.001	$(50.240 \pm 0.063) \times 10^{11}$	$1.469^{+0.028}_{-0.001} \times 10^{11}$	0.0295 ± 0.0003	0.1555	$9.444^{+0.178}_{-0.004} \times 10^{11}$	[62]
^{231}Pu	^{227}U	$[3/2^+]$	$(3/2^+)$	6.839 ± 0.020	$(4.763 \pm 2.063) \times 10^3$	$78.380^{+14.530}_{-15.240}$	0.0218 ± 0.0126	0.1528	$0.513^{+0.095}_{-0.100} \times 10^3$	[62][a]
^{235}Pu	^{231}U	$(5/2^+)$	$(5/2)^{[+]}$	5.951 ± 0.020	$(5.811 \pm 1.560) \times 10^7$	$8.497^{+2.236}_{-1.896} \times 10^5$	0.0171 ± 0.0081	0.1319	$0.644^{+0.170}_{-0.144} \times 10^7$	[62][a]
^{233}Cm	^{229}Pu	$[3/2^+]$	$[3/2^+]$	7.470 ± 0.050	27.000 ± 10.000	$1.786^{+0.960}_{-0.636}$	0.0963 ± 0.0652	0.1162	$15.367^{+8.260}_{-5.472}$	[62]
^{239}Cf	^{235}Cm	$[5/2^+]$	$[5/2^+]$	7.810 ± 0.060	$39.000^{+37.000}_{-12.000}$	$5.032^{+3.287}_{-1.968} \times 10^{-1}$	0.0174 ± 0.0134	0.0664	$7.583^{+4.954}_{-2.966}$	[77]

TABLE I. (*Continued.*)

Parent	Daughter	J_P^π	J_D^π	Q_α (MeV)	$T_{1/2}^{\exp}$ (s)	$T_{1/2}^{\mathrm{cal}}$ (without S_α) (s)	$S_\alpha^{\exp}$ [Eq. (8)]	S_α [Eq.(16)]	$T_{1/2}^{\mathrm{cal}}$ (s) (by using S_α [Eq. (16)])	References
^{245}Cf	^{241}Cm	$1/2^+$	$1/2^+$	7.258 ± 0.002	$(7.500 \pm 0.673) \times 10^3$	$54.425^{+1.494}_{-1.338}$	0.0073 ± 0.0008	0.0111	$4.924^{+0.135}_{-0.121} \times 10^3$	[64]
^{241}Es	^{237}Bk	$(3/2^-)$	$(3/2^-)$	8.250 ± 0.020	$8.000^{+6.000}_{-5.000}$	$4.135^{+0.682}_{-0.602} \times 10^{-2}$	0.0091 ± 0.0068	0.0465	$0.890^{+0.147}_{-0.130}$	[78]
^{243}Es	^{239}Bk	$(7/2^+)$	$(7/2^+)$	8.072 ± 0.010	21.000 ± 5.000	$1.509^{+0.130}_{-0.120} \times 10^{-1}$	0.0078 ± 0.0025	0.0309	$4.878^{+0.420}_{-0.388}$	[79,80][b]
^{251}Es	^{247}Bk	$(3/2^-)$	$(3/2^-)$	6.598 ± 0.003	$(2.420 \pm 0.598) \times 10^7$	$1.090^{+0.037}_{-0.037} \times 10^5$	0.0048 ± 0.0013	0.0051	$2.149^{+0.073}_{-0.073} \times 10^7$	[64]
^{253}Es	^{249}Bk	$7/2^+$	$7/2^+$	6.739	$(1.769 \pm 0.003) \times 10^5$	2.263×10^4	0.0128	0.0124	18.277×10^5	[62]
^{251}No	^{247}Fm	$7/2^+$	$7/2^+$	8.752 ± 0.004	0.800 ± 0.010	$1.124^{+0.041}_{-0.034} \times 10^{-2}$	0.0141 ± 0.0006	0.0070	$1.602^{+0.058}_{-0.048}$	[62]
^{253}Lr	^{249}Md	$(7/2^-)$	$(7/2^-)$	8.918 ± 0.020	$(6.320 \pm 0.460) \times 10^{-1}$	$8.611^{+1.366}_{-1.129} \times 10^{-3}$	0.0140 ± 0.0030	0.0114	$7.548^{+1.197}_{-0.990} \times 10^{-1}$	[62]
^{263}Sg	^{259}Rf	$[7/2^+]$	$[7/2^+]$	9.400 ± 0.060	0.940 ± 0.140	$3.508^{+1.752}_{-1.161} \times 10^{-3}$	0.0044 ± 0.0022	0.0089	$0.396^{+0.198}_{-0.131}$	[62]
^{265}Hs	^{261}Sg	$[3/2^+]$	$[3/2^+]$	10.470 ± 0.015	$(1.960 \pm 0.160) \times 10^{-3}$	$2.219^{+0.174}_{-0.223} \times 10^{-5}$	0.0114 ± 0.0019	0.0096	$2.315^{+0.182}_{-0.233} \times 10^{-3}$	[62]
^{269}Hs	^{265}Sg	$[9/2^+]$	$[9/2^+]$	9.315 ± 0.022	$9.700^{+9.700}_{-3.300}$	$3.499^{+0.547}_{-0.558} \times 10^{-2}$	0.0039 ± 0.0024	0.0184	$1.900^{+0.297}_{-0.303}$	[81]
^{281}Ds	^{277}Hs	$[3/2^+]$	$[3/2^+]$	8.856 ± 0.030	$1.400^{+5.100}_{-0.900} \times 10^2$	$7.364^{+1.978}_{-1.513}$	0.0979 ± 0.0889	0.0248	$2.971^{+0.798}_{-0.610} \times 10^2$	[5]
^{272}Rg	^{268}Mt	$[5^+,6^+]$	$[5^+,6^+]$	11.150 ± 0.035	$(3.800^{+1.400}_{-0.800}) \times 10^{-3}$	$4.882^{+1.035}_{-0.855} \times 10^{-6}$	0.0014 ± 0.0006	0.0084	$0.580^{+0.123}_{-0.102} \times 10^{-3}$	[80]
^{289}Fl	^{285}Cn	$[5/2^+]$	$[5/2^+]$	9.970 ± 0.050	2.400 ± 0.600	$8.551^{+3.335}_{-2.552} \times 10^{-2}$	0.0432 ± 0.0230	0.0152	$5.618^{+2.191}_{-1.677}$	[62]

[a]The partial half-life is calculated by using the half-life and the intensity given in Ref. [62] by taking account of the uncertainty in both.
[b]The mentioned partial half-life is an average of the ones from the indicated references.

TABLE II. The quadrupole (β_2), octupole (β_3), hexadecapole (β_4), and hexacontatetrapole (β_6) deformations of the deformed daughter nuclei which were involved in the decays presented in Table I [82].

Nucleus	β_2	β_3	β_4	β_6	Nucleus	β_2	β_3	β_4	β_6	Nucleus	β_2	β_3	β_4	β_6
^{171}Pt	0.126		−0.003	−0.001	^{195}At	−0.215			−0.001	^{229}Th	0.190		0.114	0.020
^{175}Pt	0.180		0.004	−0.004	^{196}At	−0.207		0.001	−0.001	^{227}U	0.182		0.121	0.031
^{179}Pt	0.274		0.003	−0.009	^{197}At	−0.207		0.001	−0.001	^{231}U	0.198		0.115	0.017
^{181}Pt	0.265		−0.015	−0.009	^{198}At	−0.207		−0.007	−0.001	^{229}Pu	0.190		0.114	0.024
^{173}Au	−0.105		−0.011	− 0.001	^{199}At	0.080		0.002	−0.002	^{235}Cm	0.215		0.102	0.001
^{175}Au	−0.122		−0.010	0.001	^{200}At	0.089		−0.006	−0.001	^{241}Cm	0.223		0.087	−0.022
^{187}Hg	−0.139		−0.024		^{201}At	0.071		−0.007	−0.001	^{237}Bk	0.215		0.093	−0.007
^{213}Pb	0.009	−0.055	0.009	0.001	^{202}At	0.062		−0.007	0.001	^{239}Bk	0.215		0.093	−0.012
^{192}Bi	−0.052		0.009		^{204}At	−0.053		−0.007	0.002	^{247}Bk	0.235		0.048	−0.034
^{193}Bi	−0.052		0.009		^{215}At	0.018		0.016	−0.001	^{249}Bk	0.235		0.040	−0.037
^{194}Bi	−0.052		0.009		^{199}Rn	−0.207		0.001	−0.001	^{247}Fm	0.234	–	0.057	−0.038
^{195}Bi	−0.052		0.009		^{201}Rn	−0.199		−0.016	−0.001	^{249}Md	0.235		0.040	−0.036
^{196}Bi	−0.052		0.009	−0.001	^{205}Rn	−0.079		0.002	0.003	^{259}Rf	0.239		−0.025	−0.032
^{197}Bi	−0.052		0.009	0.001	^{207}Rn	−0.053		−0.007	−0.001	^{261}Sg	0.238		−0.025	−0.031
^{198}Bi	−0.052		0.009	0.001	^{218}Fr	0.050	0.154	0.029	0.008	^{265}Sg	0.229		−0.053	−0.020
^{204}Bi	−0.044		0.009	0.001	^{223}Fr	0.146	−0.135	0.109	0.008	^{277}Hs	0.145		−0.049	−0.006
^{191}Po	0.275		−0.031	−0.004	^{219}Ac	0.020	−0.099	0.011	0.004	^{268}Mt	0.221		−0.071	−0.014
^{193}Po	−0.215		0.009	0.002	^{223}Ac	0.147	−0.151	0.110	0.010	^{285}Cn	0.089		−0.037	0.003
^{195}Po	0.071		0.002	−0.001	^{227}Ac	0.172	−0.105	0.112	0.007					
^{197}Po	0.062		0.001	−0.002	^{225}Th	0.165	−0.137	0.112	0.010					

Figure 1 shows the variation in the estimated preformation probability for the even(Z)-odd(N) isotopes of Hg($Z = 80$), Po($Z = 84$), U($Z = 92$), Pu($Z = 94$), and Hs($Z = 108$) with the neutron number (N) of the decaying parents. For comparison, the results for the corresponding even-even isotopes taken from Ref. [26] are added. The presented even-odd results confirm the periodic behavior detected [26] for the preformation probability as a function of the neutron and charge numbers with consecutive local maxima and minima. The results shown in Fig. 1 indicate the presence of local minima at $N = 104(102)$ and $N = 126$. These minima are related to the neutron-shell and subshell closures. Local maxima are indicated at $N = 96, 112$, and 134(136). It is also interesting to note from Fig. 1 that, along the different isotopic chains, the α-preformation probability inside the even-odd nucleus is less than that of its even-even neighboring isotopes. While the maximum preformation probability inside an even-even nucleus displayed in Fig. 1 is 0.1900 ± 0.0800

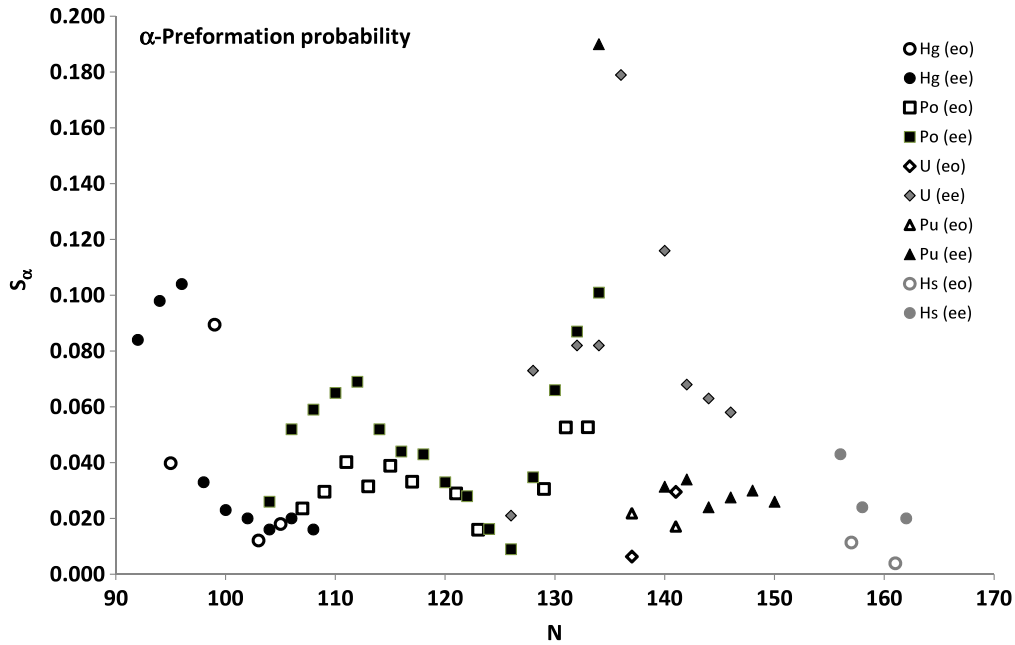

FIG. 1. (Color online) The estimated α-preformation probability Eq. (8) inside even(Z)-odd(N) and even(Z)-even(N) nuclei belong to several isotopic chains versus the neutron number of parent nuclei. The data for the even-even isotopes are taken from Ref. [26].

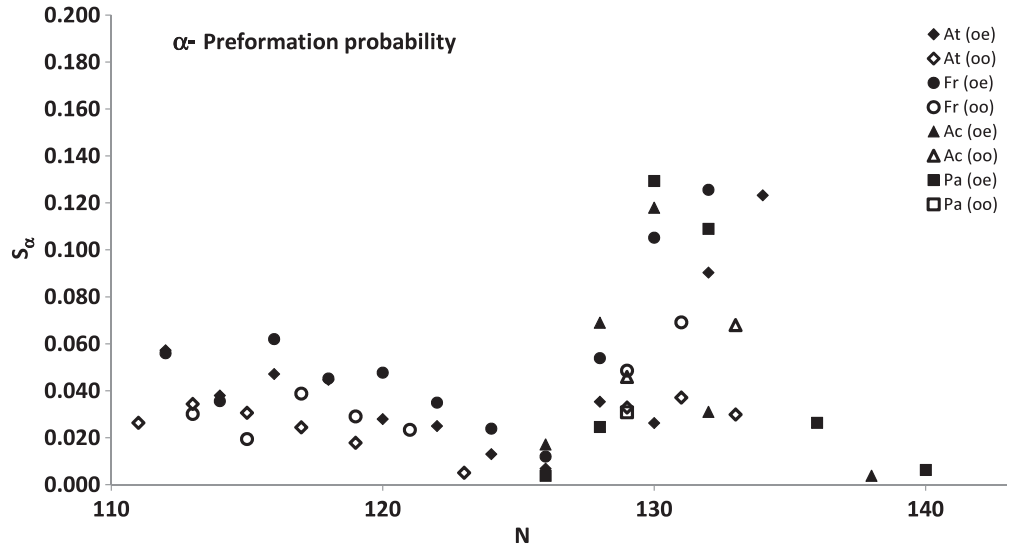

FIG. 2. The same as Fig. 1 but for odd(Z)-even(N) and odd(Z)-odd(N) isotopes.

(^{228}Pu) [26], the maximum ones for the even-odd isotopes in the same figure are 0.0895 ± 0.0307 (^{179}Hg) and 0.0527 ± 0.0018 (^{217}Po). The range of the estimated α-preformation probability inside all mentioned 44 even-odd nuclei lies between 0.0039 ± 0.0024 (^{269}Hs) and 0.0979 ± 0.0889 (^{281}Ds). Figure 2 displays the deduced preformation probability for the odd(Z)-even(N) and odd(Z)-odd(N) At($Z = 85$), Fr($Z = 87$), Ac($Z = 89$), and Pa($Z = 91$) isotopes as a function of their neutron numbers. The obtained periodic behavior of the presented S_α in Fig. 2 with N confirms the local minimum associated with the shell closure at $N = 126$. A local maximum around $N = 116$ is indicated. The obtained preformation probabilities of α in the odd-odd nuclei are always smaller than those of the close odd-even neighbors that belong to the same isotopic chain. The deduced α-preformation probabilities in the studied 41 odd-even nuclei are ranged from 0.0005 to 0.1294 ± 0.0539. The obtained ones inside the mentioned 20 odd-odd nuclei are in the range between 0.0014 ± 0.0006 (^{272}Rg) and 0.0692 ± 0.0421 (^{218}Fr).

The deduced α-preformation probability in the odd(Z)-even(N) isotones of $N = 112$, 124, 126, 130, and 132 is plotted as a function of the parent charge number (Z) in Fig. 3. In the same figure, the presented results for the odd-even isotones are compared with those of the associated even-even ones, which are taken from Ref. [26]. Like isotopes, the α-preformation probabilities in odd-even isotones are less than the ones in their even-even neighbors along the same isotonic chain. The maximum preformation

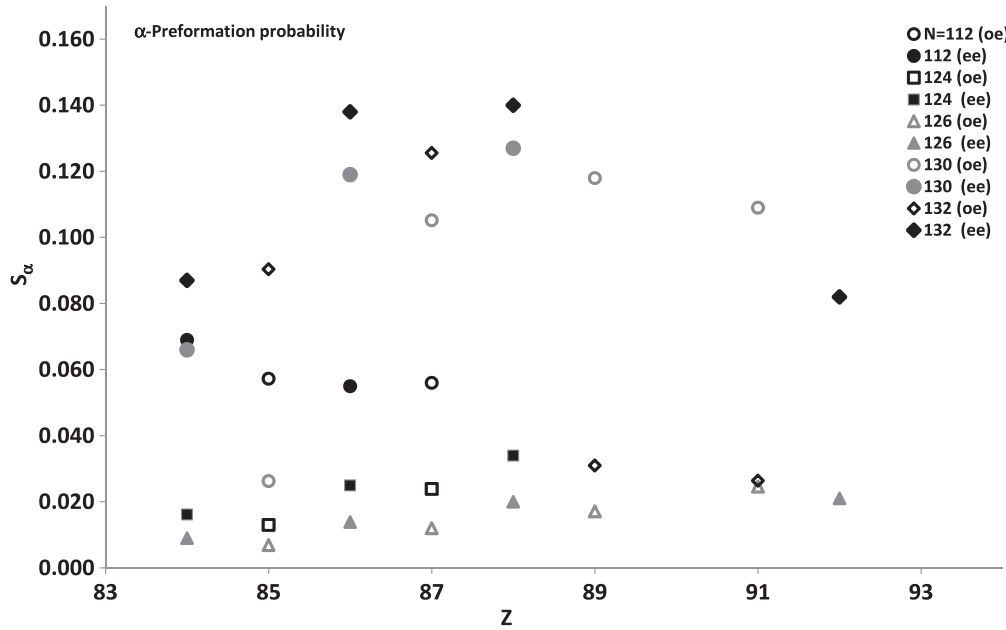

FIG. 3. The estimated α-preformation probability Eq. (8) inside odd(Z)-even(N) and even(Z)-even(N) nuclei belong to several isotonic chains versus the charge number of parent nuclei. The data for the even-even isotopes are taken from Ref. [26].

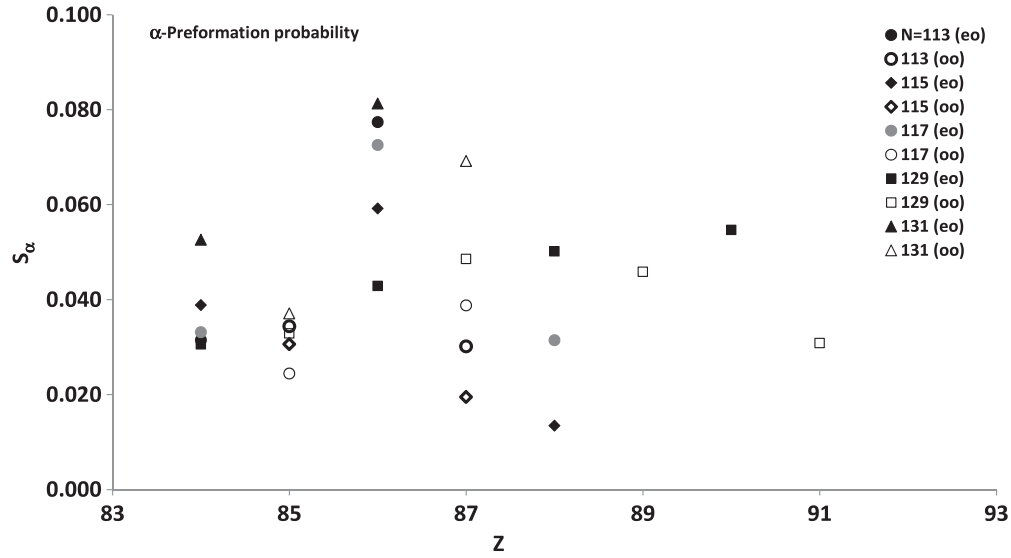

FIG. 4. The same as Fig. 3 but for even(Z)-odd(N) and odd(Z)-odd(N) isotones.

probability in an even-even isotone presented in Fig. 3 is 0.1400 ± 0.0270 [^{220}Ra($N = 132$)] [26], whereas the maximum one in an odd-even isotone in the same figure is 0.1256 ± 0.0147 [^{219}Fr($N = 132$)]. Figure 4 shows the estimated α-preformation probability inside the $N = 113, 115, 117, 129$, and 131 even(Z)-odd(N) and odd(Z)-odd(N) isotones versus the charge numbers of the parent nuclei. Again, the deduced α-preformation probability inside odd-odd isotones is lower than in the even-odd isotonic neighbors. The maximum S_α inside an even-odd isotone displayed in Fig. 4 is 0.0813 ± 0.0087 [^{217}Rn($N = 131$)]. The maximum presented one in the same figure for an odd-odd isotone is 0.0692 ± 0.0421 [^{218}Fr($N = 131$)].

However, the pairing of the nucleons in the nucleus influences the α-preformation probability inside it. This would be clearly seen when we look at the nuclei of closest neighbors. For instance, the estimated α-preformation probabilities inside the $^{218}_{132}\mathrm{Rn}_{86}(ee)$, $^{217}_{130}\mathrm{Fr}_{87}(oe)$, $^{217}_{131}\mathrm{Rn}_{86}(eo)$, and $^{218}_{131}\mathrm{Fr}_{87}(oo)$ neighbors, respectively, are $S_\alpha(\alpha + {}^{214}\mathrm{Po}) = 0.1380$ [26], $S_\alpha(\alpha + {}^{213}\mathrm{At}) = 0.1052$, $S_\alpha(\alpha + {}^{213}\mathrm{Po}) = 0.0813$, and $S_\alpha(\alpha + {}^{214}\mathrm{At}) = 0.0692$. Confirming the results discussed above, the α preformation inside the even-even ^{218}Rn nucleus has the highest probability among its neighbors. The α-preformation probability decreases in ^{217}Fr due to the effect of the unpaired proton outside the proton closed shell of $Z = 82$. The effect of the unpaired neutron outside the neutron-shell closure of $N = 126$ in ^{217}Rn, which decreases the probability of the α preformation inside it, is greater than the one of the unpaired proton in ^{217}Fr. The ^{218}Fr nucleus has the smallest α-preformation probability, relative to its neighbors, under the effect of two unpaired nucleons, proton and neutron. Moreover, the detailed calculations show a minor correlation between the preformation probability and the difference between the position of the lowest point (r_{min}) of the pocket in the internal region of the α + daughter interaction potential and the first turning point (r_1). The values of $r_{\mathrm{min}} - r_1$ for the mentioned ^{218}Rn, ^{217}Fr, ^{217}Rn, and ^{218}Fr nuclei, respectively, are 1.05, 1.04, 1.04, and 1.02 fm. This means that the preformation probability is directly proportional to the quantity $r_{\mathrm{min}} - r_1$.

To place the present results in context, a relevant pairing term (a_p) is added to the empirical expression given by Eq. (9) to account for the pairing influences on the α-preformation probability in the open-shell nuclei,

$$S_\alpha = Ae^{-\alpha(Z-Z_0-Z_c)^2}e^{-\beta(N-N_0-N_c)^2} - a_p, \quad a_p = \begin{cases} 0.0041\,(Z-Z_0)^{1/3} & \text{for odd}(Z)\text{-even}(N)\ \text{nuclei}, \\ 0.0051\,(N-N_0)^{1/3} & \text{for even}(Z)\text{-odd}(N)\ \text{nuclei}, \\ 0.0082\,(Z-Z_0+N-N_0)^{1/3} & \text{for odd}(Z)\text{-odd}(N)\ \text{nuclei}. \end{cases} \quad (16)$$

The fitting parameters of Eq. (16) as obtained in Ref. [26] are summarized in Table III. For the sets of the proton-, neutron-shell, and subshell closures of $(Z_0, N_0) = (82,126)$, $(82,152)$, and $(102,126)$, improved values of $A = 0.204, 0.223$, and 0.180, respectively, are adopted instead of the values given in Ref. [26]. These values are obtained from the fit for the present results of the preformation probability in addition to the results obtained in the mentioned reference.

Returning to Table I, the obtained preformation probabilities for the studied decays based on the modified empirical formula Eq. (16) are presented in the ninth column. The calculated half-lives upon these preformation probabilities are listed in the tenth column of the same table. As seen in Table I, for the mentioned 41 odd(Z)-even(N) nuclei, the estimated values of the preformation probability inside 34 nuclei (83%) by using Eq. (16) are fairly consistent with those deduced from Eq. (8). The obtained preformation probability

TABLE III. The fitting parameters of the empirical formula for the α-preformation probability Eq. (16) taken from Ref. [26].

Z_0	N_0	Z_c	α	N_c	β	A
50	82	10	0.0231	8	0.0126	0.341
70	82	6	0.0066	8	0.0126	0.092
	102			10	0.0090	0.029
82	82	8	0.0126	8	0.0126	0.311
	102			10	0.0090	0.105
	126			12	0.0159	0.204[a]
	152			16	0.0064	0.223[a]
102	126	10	0.0020	12	0.0159	0.180[a]
	152			16	0.0064	0.041

[a]The value given in Ref. [26] is changed upon considering the present data in the fitting process.

for 9 nuclei out of these 34 ones are already within the experimental values, taking into account the uncertainty range. In addition, for nine cases the typical difference between the estimated preformation probability based on Eq. (16) and the one deduced from the experimental data Eq. (8) is less than 0.01. The obtained minimum percentage difference by taking into account the uncertainty range between the two estimated values for the other 16 nuclei is less than 75%. The percentage difference between the two estimated values is greater than 75% for only seven nuclei. Upon the mentioned criteria, the preformation probabilities estimated by using Eq. (9), without the relevant pairing term, are consistent with the values deduced by Eq. (8) for 32 nuclei (78%) out of the considered 41 odd-even ones. Actually, the obtained half-life based on the preformation probability given by Eq. (16) is approximately two orders of magnitude less than the experimental one only for three nuclei (^{227}Ac, ^{227}Pa, and ^{231}Pa). The standard deviation $\sigma = \sqrt{\sum_{i=1}^{n} [\log_{10}(T_{1/2}^{\rm cal}/T_{1/2}^{\rm exp})]^2/(n-1)}$ of the calculated half-lives of the mentioned odd-even nuclei based on S_α [Eq. (16)] with respect to the experimental ones is improved from 0.616 to 0.597 after adding the pairing term to Eq. (9), taking account of the uncertainty range. If we excluded the anomalous results of the mentioned three nuclei, the calculated standard deviation improves from 0.282 to 0.249 upon adding the pairing term. On the other hand, among the 44 even(Z)-odd(N) nuclei considered here, the obtained values of the preformation probability from Eq. (16) for 36 nuclei (82%) appear to be consistent with the values deduced by using Eq. (8). For 9 nuclei out of these 36 ones, the deduced preformation probability is indeed within the experimental value. The obtained typical difference between the two values is less than 0.01 for 14 cases whereas the percentage difference between them is less than 75% for the remaining 13 cases. Only for nine nuclei is the percentage difference between the two obtained values greater than 75%. Without introducing the pairing term, the deduced preformation probability that uses Eq. (9) is consistent with the estimated values by Eq. (8) for 30 nuclei (68%). For ^{229}U only, the calculated half-life time based on the preformation probability deduced by Eq. (16) is two orders of magnitude smaller than the experimental one. Upon adding the pairing term to Eq. (9), the standard deviation of the calculated half-lives based on S_α [Eq. (16)] improves from $\sigma = 0.446$ to $\sigma = 0.411$. If we remove the calculated half-life of ^{229}U from computing the standard deviation, it becomes $\sigma = 0.347$. Finally, for 20 studied odd(Z)-odd(N) nuclei, the deduced preformation probabilities by Eq. (16) in 18 nuclei (90%) and those obtained from Eq. (8) are consistent with each other. The obtained preformation probability for 4 nuclei out of these 18 are within the experimental range. While the difference between the obtained preformation probability using Eq. (16) and the one yielded from Eq. (8) is less than 0.01 for five nuclei, the percentage difference between the two values for the remaining nine nuclei is less than 75%. Only for ^{202}Fr and ^{218}At is the minimum percentage difference between the two deduced values of the preformation probability greater than 75%. By using Eq. (9), the obtained preformation probabilities of only seven odd-odd nuclei (35%) are consistent with the values deduced by Eq. (8). Adding the pairing term to Eq. (9) improves the standard deviation of the calculated half-life times based on S_α [Eq. (16)] from $\sigma = 0.482$ to $\sigma = 0.306$.

IV. CONCLUSION

The α-preformation probability inside 105 odd(Z)-even(N), even(Z)-odd(N), and odd(Z)-odd(N) open-shell nuclei in the region of $80 \leqslant Z \leqslant 114$ and $95 \leqslant N \leqslant 175$ is studied. The influence of contributing unpaired pairs of protons and neutrons to the formed α particle on its preformation probability inside parent nuclei has been investigated. Only the ground-state to ground-state decays in which the parents and daughters have the same ground-state spin and parity are considered to draw a conclusion on the pure pairing effect away from any transferred angular momentum. The calculations are performed by using a Hamiltonian energy-density scheme based on the SLy4 Skyrme-like interaction and the WKB approximation of the penetration probability. The pairing correlations are taken into account in the self-consistent Skyrme HF + BCS calculations of the density distributions of the involved nuclei. The deformations in the daughter nuclei as well as the uncertainty in both the released energy and the experimental half-lives are also considered. It is found that along the different isotopic (isotonic) chains, the α-preformation probabilities inside the even-odd (odd-even) nuclei are less than those in the even-even neighboring isotopes (isotones). Also, the α-preformation probability inside odd-odd nuclei is predicted to be less than in the even-odd and even-odd close neighbors. The empirical formula [26] that gives the α-preformation probability inside even(Z)-even(N) nuclei in terms of the numbers of protons ($Z - Z_0$) and neutrons ($N - N_0$) outside their closed shells Z_0 and N_0 has been improved by adding a relevant pairing term. This pairing term is determined by fitting the extracted α-preformation probabilities in the odd-A and odd(Z)-odd(N) open-shell nuclei. Instead of 66% (without pairing), 84% of the preformation probabilities obtained by the improved formula, upon adding the pairing term, are fairly consistent with the experimentally extracted ones.

[1] W. D. Myers and W. J. Swiatecki, Nucl. Phys. **81**, 1 (1966).
[2] A. Sobiczewski, F. A. Gareev, and B. N. Kalinkin, Phys. Lett. **22**, 500 (1966).
[3] U. Mosel and W. Greiner, Z. Phys. **222**, 261 (1969).
[4] S. Hofmann and G. Münzenberg, Rev. Mod. Phys. **72**, 733 (2000), and references therein.
[5] Ch. E. Düllmann *et al.*, Phys. Rev. Lett. **104**, 252701 (2010).
[6] J. Khuyagbaatar *et al.*, Phys. Rev. Lett. **112**, 172501 (2014).
[7] Y. T. Oganessian *et al.*, J. Phys. G **34**, R165 (2007), and references therein.
[8] Y. T. Oganessian *et al.*, Nature (London) **400**, 242 (1999).
[9] L. Stavsetra, K. E. Gregorich, J. Dvorak, P. A. Ellison, I. Dragojević, M. A. Garcia, and H. Nitsche, Phys. Rev. Lett. **103**, 132502 (2009).
[10] P. A. Ellison *et al.*, Phys. Rev. Lett. **105**, 182701 (2010).
[11] K. Morita *et al.*, J. Phys. Soc. Jpn. **76**, 045001 (2007).
[12] C. Xu, Z. Ren, and Y. Guo, Phys. Rev. C **78**, 044329 (2008).
[13] D. N. Poenaru, R. A. Gherghescu, and W. Greiner, Phys. Rev. Lett. **107**, 062503 (2011).
[14] R. Bonetti and A. Guglielmetti, Rom. Rep. Phys. **59**, 301 (2007).
[15] W. M. Seif, M. Shalaby, and M. F. Alrakshy, Phys. Rev. C **84**, 064608 (2011).
[16] M. Bhattacharya, S. Roy, and G. Gangopadhyaya, Phys. Lett. B **665**, 182 (2008).
[17] S. Peltonen, D. S. Delion, and J. Suhonen, Phys. Rev. C **75**, 054301 (2007).
[18] R. G. Lovas, R. J. Liotta, A. Insolia, K. Varga, and D. S. Delion, Phys. Rep. **294**, 265 (1998).
[19] I. Tonozuka and A. Arima, Nucl. Phys. A **323**, 45 (1979).
[20] S. M. S. Ahmed, R. Yahaya, and S. Radiman, Rom. Rep. Phys **65**, 1281 (2013).
[21] G. Dodig-Crnković, F. A. Janouch, R. J. Liotta, and L. J. Sibanda, Nucl. Phys. A **444**, 419 (1985).
[22] W. M. Seif, Phys. Rev. C **74**, 034302 (2006).
[23] M. Ismail and A. Adel, Phys. Rev. C **88**, 054604 (2013).
[24] P. E. Hodgson and E. Běták, Phys. Rep. **374**, 1 (2003).
[25] J. C. Pei, F. R. Xu, Z. J. Lin, and E. G. Zhao, Phys. Rev. C **76**, 044326 (2007).
[26] W. M. Seif, J. Phys. G **40**, 105102 (2013).
[27] K. Varga, R. G. Lovas, and R. J. Liotta, Phys. Rev. Lett. **69**, 37 (1992).
[28] P. Mohr, Phys. Rev. C **73**, 031301(R) (2006).
[29] D. N. Poenaru, W. Greiner, M. Ivascu, D. Mazilu, and I. H. Plonski, Z. Phys. A **325**, 435 (1986).
[30] D. N. Basu, J. Phys. G **29**, 2079 (2003).
[31] D. N. Poenaru, M. Ivascu, A. Sandulescu, and W. Greiner, Phys. Rev. C **32**, 572 (1985).
[32] V. G. Soloviev, Phys. Lett. **1**, 202 (1962).
[33] F. A. Janouch and R. J. Liotta, Phys. Rev. C **27**, 896 (1983).
[34] F. Catara, A. Insolia, E. Maglione, and A. Vitturi, Phys. Rev. C **29**, 1091 (1984).
[35] M. W. Herzog, O. Civitarese, L. Ferreira, R. J. Liotta, T. Vertse, and L. J. Sibanda, Nucl. Phys. A **448**, 441 (1986).
[36] M. Bhuyan, S. K. Patra, and R. K. Gupta, Phys. Rev. C **84**, 014317 (2011).
[37] X. J. Bao, H. F. Zhang, B. S. Hu, G. Royer, and J. Q. Li, J. Phys. G **39**, 095103 (2012).
[38] S. M. S. Ahmed, R. Yahaya, S. Radiman, and M. S. Yasir, J. Phys. G **40**, 065105 (2013).
[39] D. E. Ward, B. G. Carlsson, and S. Åberg, Phys. Rev. C **88**, 064316 (2013).
[40] A. N. Andreyev *et al.*, Phys. Rev. Lett. **110**, 242502 (2013).
[41] S. S. Malik and R. K. Gupta, Phys. Rev. C **39**, 1992 (1989).
[42] B. Buck, A. C. Merchant, and S. M. Perez, Phys. Rev. C **45**, 2247 (1992).
[43] C. Samanta, P. Roy Chowdhury, and D. N. Basu, Nucl. Phys. A **789**, 142 (2007).
[44] M. Ismail, W. M. Seif, and H. El-Gebaly, Phys. Lett. B **563**, 53 (2003).
[45] S. A. Gurvitz and G. Kälbermann, Phys. Rev. Lett. **59**, 262 (1987).
[46] N. G. Kelkar and H. M. Castañeda, Phys. Rev. C **76**, 064605 (2007).
[47] V. Yu. Denisov and H. Ikezoe, Phys. Rev. C **72**, 064613 (2005).
[48] F. L. Stancu and D. M. Brink, Nucl. Phys. A **270**, 236 (1976).
[49] M. Brack, C. Guet, and H.-B. Håkansson, Phys. Rep. **123**, 275 (1985).
[50] V. Y. Denisov and W. Noerenberg, Eur. Phys. J. A **15**, 375 (2002).
[51] W. M. Seif, Eur. Phys. J. A **38**, 85 (2008).
[52] P. Bonche, H. Flocard, and P. H. Heenen, Nucl. Phys. A **467**, 115 (1987).
[53] E. Chabanat, E. Bonche, E. Haensel, J. Meyer, and R. Schaeffer, Nucl. Phys. A **635**, 231 (1998).
[54] J. W. Negele and D. Vautherin, Phys. Rev. C **5**, 1472 (1972).
[55] M. Ismail and W. M. Seif, Phys. Rev. C **81**, 034607 (2010).
[56] M. Ismail, W. M. Seif, A. Y. Ellithi, and F. Salah, J. Phys. G **35**, 075101 (2008).
[57] C. Xu and Z. Ren, Phys. Rev. C **73**, 041301(R) (2006).
[58] B. Buck, J. C. Johnston, A. C. Merchant, and S. M. Perez, Phys. Rev. C **53**, 2841 (1996).
[59] K. Wildermuth and Y. C. Tang, *A Unified Theory of the Nucleus* (Academic, New York, 1977).
[60] P.-G. Reinhard, in *Computational Nuclear Physics*, edited by K. Langanke, J. A. Maruhn, and S. E. Koonin (Springer-Verlag, Berlin, 1990), Vol. 1, p. 28.
[61] M. Wang, G. Audi, A. H. Wapstra, F. G. Kondev, M. MacCormick, X. Xu, and B. Pfeiffer, Chin. Phys. C **36**, 1603 (2012).
[62] G. Audi, F. G. Kondev, M. Wang, B. Pfeiffer, X. Sun, J. Blachot, and M. MacCormick, Chin. Phys. C **36**, 1157 (2012).
[63] Y. Qian and Z. Ren, Phys. Rev. C **88**, 044329 (2013).
[64] N. Dasgupta-Schubert and M. A. Reyes, At. Data Nucl. Data Tables **93**, 907 (2007).
[65] A. N. Andreyev *et al.*, Phys. Rev. C **87**, 054311 (2013).
[66] V. R. Vanin, N. L. Maidana, R. M. Castro, E. Achterberg, O. A. Capurro, and G.V. Martí, Nucl. Data Sheets **108**, 2393 (2007).
[67] Z. Kalaninová *et al.*, Phys. Rev. C **89**, 054312 (2014).
[68] Z. Kalaninová *et al.*, Phys. Rev. C **87**, 044335 (2013).
[69] J. Uusitalo *et al.*, Phys. Rev. C **87**, 064304 (2013).
[70] J. Uusitalo *et al.*, Phys. Rev. C **71**, 024306 (2005).
[71] H. De Witte *et al.*, Eur. Phys. J. A **23**, 243 (2005).
[72] T. Enqvist, K. Eskola, A. Jokinen, M. Leino, W. H. Trzaska, J. Uusitalo, V. Ninov, and P. Armbruster, Z. Phys. A **354**, 1 (1996).
[73] M. S. Basunia, Nucl. Data Sheets **108**, 633 (2007).
[74] E. Browne and J. K. Tuli, Nucl. Data Sheets **112**, 1115 (2011).
[75] F. Hoellinger, B. J. P. Gall, N. Schulz, N. Amzal, P. A. Butler, P. T. Greenlees, D. Hawcroft, J. F. C. Cocks, K. Helariutta, P. M. Jones, R. Julin, S. Juutinen, H. Kankaanpää, H. Kettunen,

P. Kuusiniemi, M. Leino, M. Muikku, and D. Savelius, Phys. Rev. C **60**, 057301 (1999).
[76] V. Ninov, F. P. Heßberger, H. Folger, S. Hofmann, A. G. Popeko, A. V. Yeremin, A. N. Andreyev, and S. Ŝaro, Proceedings of the International Conference on Exotic Nuclei and Atomic Masses ENAM-95, 571 (1995).
[77] E. Browne, Nucl. Data Sheets **98**, 665 (2003).
[78] M. J. Martin, Nucl. Data Sheets **106**, 89 (2005).
[79] S. Antalic *et al.*, Eur. Phys. J. A **43**, 35 (2010).
[80] Y. Hatsukawa *et al.*, Nucl. Phys. A **500**, 90 (1989).
[81] M. Gupta and T. W. Burrows, Nucl. Data Sheets **106**, 251 (2005).
[82] P. Möller, J. R. Nix, W. D. Myers, and W. J. Swiatecki, At. Data Nucl. Data Tables **59**, 185 (1995).